THE VORTEX RING IMPINGING ONTO A GROUND SURFACE

Taiichi Nagata
Department of Mechanical Engineering, Keio University
Yokohama 223-8522, Japan
m07492@educ.cc.keio.ac.jp

Shinnosuke Obi
Department of Mechanical Engineering, Keio University
Yokohama 223-8522, Japan
obsn@mech.keio.ac.jp

Shigeaki Masuda
Department of Mechanical Engineering, Keio University
Yokohama 223-8522, Japan
smasuda@mech.keio.ac.jp

ABSTRACT
As a part of the laboratory experiment on a microburst, the instantaneous velocity fields of an impulse-driven vortex ring impinging onto a normal wall have been investigated. The air flow has been visualized by filling ethylene glycol smoke. The instantaneous velocity fields induced by a vortex ring were measured by employing the PIV in which the cross correlation method was used.

It was shown the interactions between primary vortex ring and induced secondary vortex ring. The horizontal and vertical velocity distribution across the vortex core was discussed. The time evolution of circulation in vertical cross section can be fitted to the theoretical equation for that of incompressible viscous vortex. These results were validated by comparison with the atmospheric microburst.

INTRODUCTION
The microburst is one of the severe local storms. Previous observational studies (Fujita, 1985) (Wilson et al., 1984) demonstrated that the vortex ring produced by a downdraft played an important role in the development of flow fields near ground. Wilson et al. (1984) also suggested that the velocity field was asymmetric by 3D Doppler radar analysis. However, since it occurs randomly in space and time and it is limited in the special and time resolution, the details of the flow field associated with a natural microburst are not yet clear. So that the laboratory simulations are need for detail understanding.

The numerical study was made by Proctor (1988). It was shown that the secondary vortex ring was generated on the ground by the influence of the primary vortex ring. However, there was a lack of data of physical events to validate the numerical model. Since the axisymmetric model was used in his study, the asymmetry of horizontal velocity field was not discussed.

The experimental study was made by Alahyari et al. (1995). The microburst flow field was simulated by releasing a heavy liquid into a less dense ambient surrounding. They supposed that the cause of an asymmetry of horizontal velocity field was the circumferential instability of the vortex ring. However detailed understanding of the interaction between the vortex ring and these structures is still lacking. The asymmetry of horizontal wind structure and the vertical structure of the out flow are the important features of the microburst and the vortex ring is deeply concerned with it.

We proposed the impulse-driven vortex ring impinging onto a ground surface as the laboratory experiment on a microburst. In the previous study (Nagata et al. 2000), the horizontal and vertical cross-section of the velocity fields has been measured by employing PIV. It was shown that the development of velocity fields induced by vortex ring near the ground indicated the abrupt changes of wind directions, which can be related to the development of the secondary- and tertiary vortex rings.

In the present study, the additional analysis related with the atmospheric microburst was discussed.

EXPERIMENTAL PROCEDURE
The experimental apparatus is illustrated in figure 1. Vortex rings are generated by the impulsive motion of a speaker corn that drives the airflow through an orifice of diameter D_0=50mm.

Ethylene glycol smoke is filled both in the cylindrical chamber and the test section beforehand and is illuminated by short arc strobe light sheet of 5mm thick for obtaining the horizontal cross-sectional view near the ground. For the vertical view, 25mW He-Ne laser sheet of 2mm thick is employed because better contrast images are necessary for image processing. Images of the flow fields are captured by using CCD video camera, having 640×480 pixel

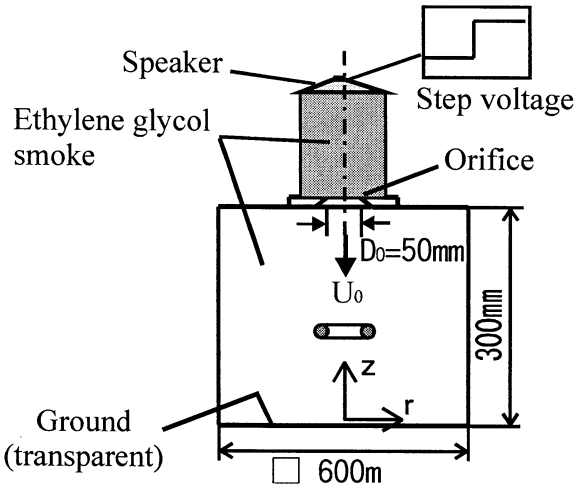

Fig.1 Experimental apparatus

arrays and 30 frames per second. The cross correlation method was used to measure displacement vectors from two successive images (Raffel et al., 1998).

The diameter of the orifice, D_0, and the initial traveling velocity of vortex ring, U_0, is taken as the references. Thus, the Reynolds number Re_0 is defined as U_0D_0/ν, ν denoting the kinematic viscosity of the air. The distance from the orifice to the ground H is $6D_0$.

RESULTS

Core trajectory

Figure 2 shows trajectories of cores of primary and secondary vortex rings. Reynolds number is 1150. These trajectories of cores were estimated from visualization images of vertical cross section. At the height Y/R0>1.30, the primary vortex core descends straightly toward the ground. It begins to move gradually outward before impingement owing to the interaction with the ground. After the impingement, it expands outward rapidly and moves away from the ground, showing the rebound. After a short pause at t*=0.72~1.07, the primary core begins to move again downward but the outward motion slows down until it stops at t*=3.58.

At the moment of restart of primary vortex (t*=1.07), the secondary vortex first observed at the upper right of the primary vortex core. It turns a round the primary one. Walker et al. (1987) and Yamada et al. (1982) found that the rebound is a consequence of the induced velocity by the secondary vortex. If it is true, the first occurrence and the initial movement of the secondary vortex can be presumed as shown by the dash-dotted line in the figure.

Figure 3 shows the core trajectory for Reynolds number of 800. As to the primary vortex, the qualitative agreement with the higher Reynolds number is

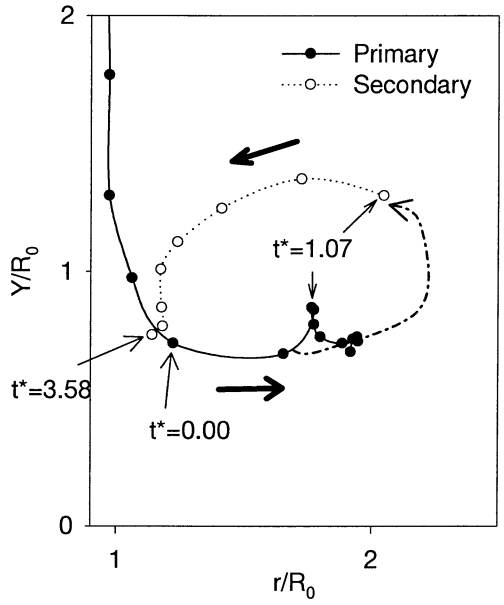

Fig.2 Trajectories of cores of the primary and the secondary vortex rings for Re_0=1150. ●;primary, ○;secondary. $t^*=t/(D_0/U_0)$. t*=0 means the moment of impingement, Δ t*=0.36.R_0: radius of the vortex ring.

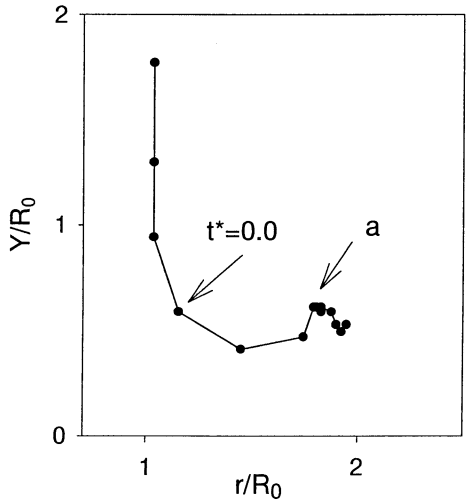

Fig.3 Trajectory of cores of the primary vortex rings for Re_0=800. $t^*=t/(D_0/U_0)$. t*=0 means the moment of impingement Δ t*=0.26.R_0: radius of the vortex ring.

obvious, but the secondary vortex can not be recognized in the video picture.

Proctor (1988) has reported the numerical simulation of an atmospheric microburst. His Reynolds number was 1.7×10^9, being six order higher than the present experiment. The time span of his simulation was t*<0.3, being much shorter than present experiment. The primary and the secondary vortex rings

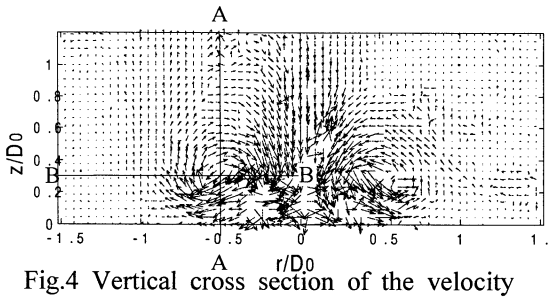

Fig.4 Vertical cross section of the velocity field; Re_0=800, times $t^* = t/(D_0/U_0)$ =0.0. (Nagata et al., 2000)

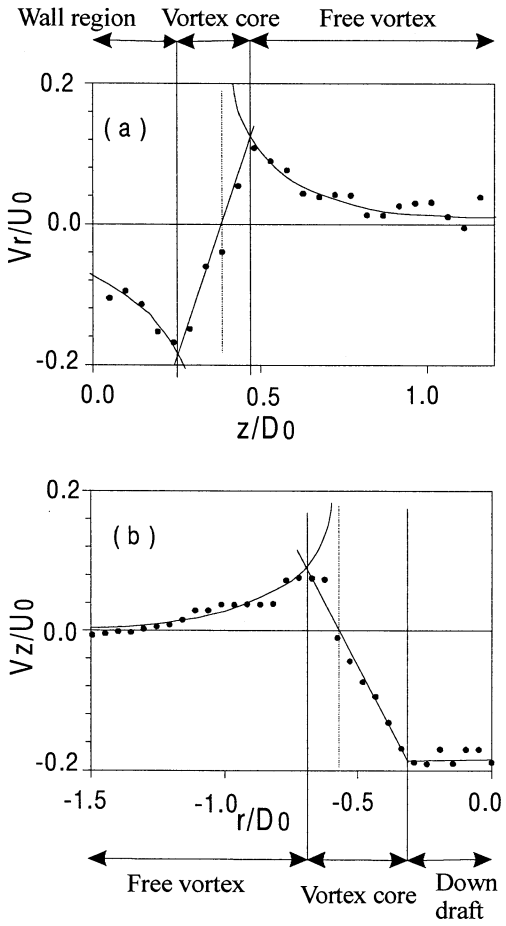

Fig.5 Velocity distributions across the vortex core at t*=0.0. (a) Horizontal velocity in vertical cross section. (b) Vertical velocity in horizontal cross section.

were observed also in his simulation, but the latter stays near the ground and doesn't travel around the former. The difference may be attributed to the difference of Reynolds number or the shortage of time of his observation.

Vertical cross section

Figure 4 shows the typical example of the instantaneous velocity vector map in a vertical cross section for Re_0=800 at t*=0. Details of the time evolution have been discussed in Nagata et al. (2000). A pair of counter-rotating circulatory streamlines can be seen, the center of which is located at r=0.6D_0 and z=0.3D_0. The downward flow is observed in the central region. This may be the trace of the vortex ring passed by. Above the vortex ring, surrounding fluid is entrained into the vortex. In the region $r/D_0>1$, the vortex ring does not induce any flows. In the Procter's simulation, the position of the vortex core was located at z=0.13D_0 and r=0.45D_0, both being comparable to the present result. The central downward flow as well as the entrainment above the ring agrees qualitatively with numerical simulation in spite of the large difference in the conditions.

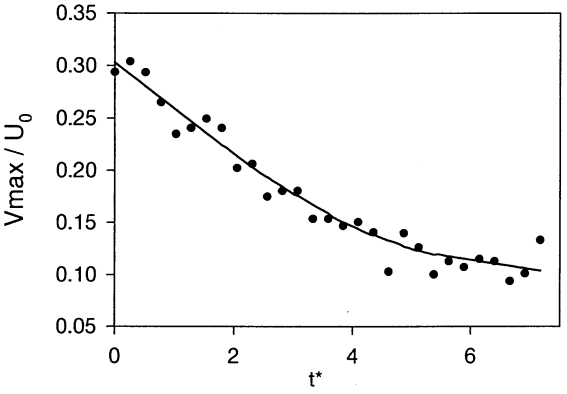

Fig. 6 The time evolution of the maximum absolute velocity in vertical cross section at Re_0=800. Times $t^* = t/(D_0/U_0)$.

Figure 5(a) shows the horizontal velocity along the vertical line A-A passing through the center of the vortex core as illustrated in figure 4. The velocity profile is divided into three regions: 1) core region in which the velocity increases linearly with z, 2) free vortex region in which the velocity decreases inversely proportional to the distance, and 3) wall region which exists between the core region and the ground. The velocity profile in the core region is asymmetric and the center of the core is deflected upward.

The vertical velocity profile along the horizontal line B-B given in figure 5(b) shows the region of downdraft in addition to the core and the free vortex regions. The vertical velocity is almost constant in the downdraft region. The center of the core is deflected outward. Although these pictures are instantaneous, the time series of video pictures indicate the same trends of the deflection of vortex core.

The vertical velocity in the downdraft region is 0.19U_0. Wilson et al. (1984) reported the measured results in the natural microburst but they did not report the magnitude of the reference velocity. So the direct comparison is impossible. If the reference velocity is assumed to be equal to the Procter's simulation, the maximum downdraft velocity in

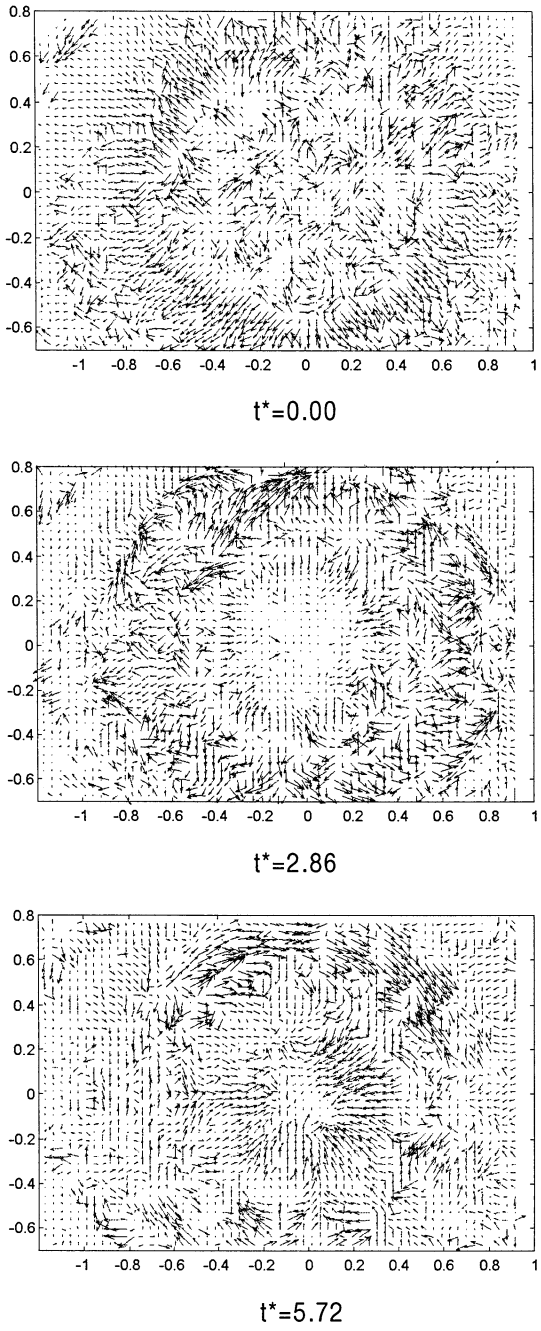

Fig. 7 Horizontal cross section of velocity field. $z \approx 0.1D_0$; Re_0=1150, H=$6D_0$, times $t^*=t/(D_0/U_0)$, (Nagata et al., 2000)

Wilson's observation amounts to $1.2U_0$. From figure 5 (a) and (b), the diameter of a vortex core is estimated to be $0.241D_0$ in horizontal direction, and $0.386D_0$ in vertical direction, that is, the vortex core is compressed in vertical direction. Neither the numerical simulation by Procter (1988) nor the natural observation by Wilson (1984) reported on the core diameter.

Figure 6 shows the evolution of the maximum absolute velocity V_{max} in the vertical cross section. The

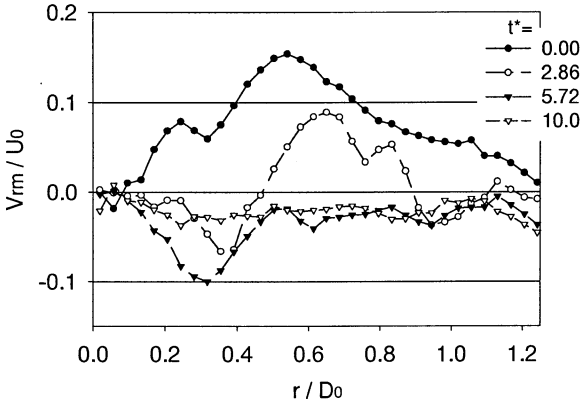

Fig.8 Circumferentially averaged radial velocity, Vrm/U_0 vs. r/D_0; Re_0=1150, $z \approx 0.1D_0$

peak value is $0.3U_0$ at the moment of impingement and it decreases monotonically with time. 30% of U_0 seems too small, while the Procter's simulation shows $2U_0$ typically. The reason of this difference remains still an open issue.

Horizontal cross section

Figure 7 shows the horizontal cross section of the instantaneous velocity fields near the ground ($z/D_0 \approx 0.1$) after impingement. At the beginning (t*=0.00), most of the velocity vectors are in the radial outward direction and the flow seems axisymmetric. At t*=2.86, the vector field shows three concentric circular regions. The vectors in the innermost region are direct inward. In the intermediate region, they are direct radially outward and in the outermost region they are direct inward again. These may be due to the secondary, the primary and the tertiary vortex ring. At t*=5.72, the axisymmetric pattern is broken up and clusters of velocity vector appear in the center region. This outward flow is one of the characteristic features in the natural microburst as observed by Wilson et al. (1984). Because of the limited spatial resolution, however, the three concentric circular regions, the asymmetry and the cluster shown here are not obvious in the natural observations.

The circumferentially averaged radial velocity

$$V_{rm} = \int_0^{2\pi} V_r \, d\theta \Big/ 2\pi \qquad (1)$$

at $z/D_0 \approx 0.1$ is plotted against radial position in figure 8. At t*=0.00, velocities are wholly in radially outward direction. At t*=2.86, there are two successive changes in radial direction, inward – outward – inward. At t*=5.72, the radial outward flow disappears while the radial inward flow remains strong near the center region. At t*=10.0, the radial inward velocity decreases bellow 4% of U_0. In natural microbursts, t he gravity drives the strong downdraft

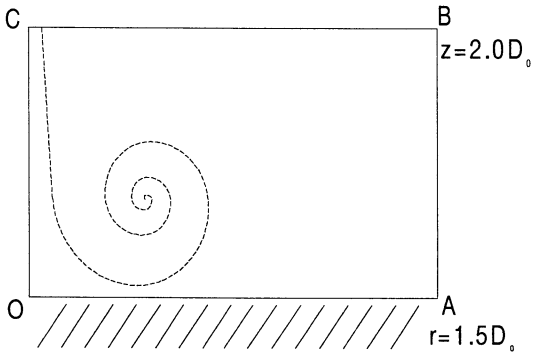

Fig. 9 The closed circuit for the line integral.

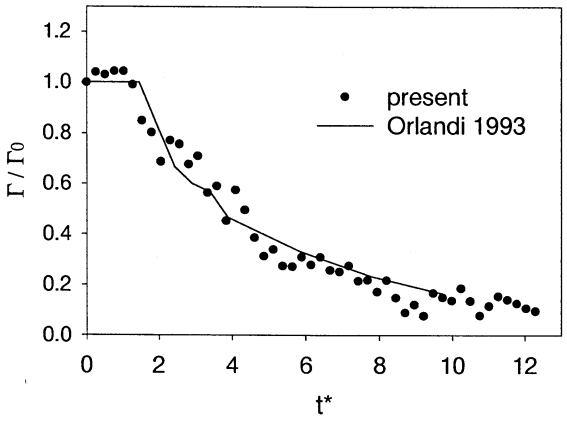

Fig.10 Time evolution of circulation,Γ/Γ_0.Γ_0: Initial circulation. $t^*=t/(D_0/U_0)$

and resulting radial outflow dominates the wind field (Wilson, 1984). If it is assumed that the flow presented in figure 8 is superposed on the gravity driven radial outflow, an aircraft moving across a downburst experiences successive change of head wind.

Wilson et al. reported the wind shear, which is defined as the temporal maximum of the velocity gradient in the horizontal direction. Figure 8 indicates that the radial distribution of wind shear is strongly dependent on time. This kind of information is essentially important for the aircraft operation.

Lifetime

In order to know the lifetime of the vortex ring, we have estimated the total circulation defined as,

$$\Gamma \equiv \oint v ds \qquad (2)$$

, in which the line integral is performed along the closed circuit OABC as illustrated in figure 9, and ds and v are the line element and velocity component along the circuit respectively.

Figure 10 shows the time evolution of the circulation. It remains nearly constant at the initial stage of impingement ($t^*<1.0$) and then decreases monotonically in time. The present result is in good agreement with the DNS data by Orlandi (1993) given by the solid line in figure 10. He presented the three dimensional DNS of the isolated vortex ring impinging onto the flat plate. The time evolution of circulation for incompressible viscous vortex flow in free space is expressed as,

$$\frac{\Gamma}{\Gamma_0} = 1 - \exp\left(\frac{-C\,\mathrm{Re}_0}{t^*}\right) \qquad (3)$$

where C is a constant (McCormack, 1973). By replacing t^* with $t^* - t^*_c$, where t^*_c is the time when Γ begins to decrease, and by fitting the data in figure 10, the constant is estimated as $C = 1.35\times10^{-3}$ for present case and $C = 1.11\times10^{-3}$ for DNS (Orlandi, 1993). Using this equation (3), the time required for Γ to decrease bellow 10% of the initial value is estimated as $t^*=17.4$. Wilson et al. (1984) demonstrated that the average lifetime of atmospheric microbursts are about 10 minutes, which corresponds to $t^* \approx 1.56$. The present result shows poor agreement with natural microbursts.

Concluding remarks

As a part of the laboratory experiments on a microburst, instantaneous velocity fields around an impulsively started constant density vortex ring impinging perpendicularly onto a ground were investigated.

The trajectories of cores of primary and secondary vortex rings were observed. The former showed the rebound and the latter traveled around the former. These behaviors were not observed in the numerical simulation (Proctor, 1988). The difference may be attributed to the difference of Reynolds number or the shortage of time of his observation.

The horizontal velocity profile through the center of the vortex core was divided into three regions: 1) core region, 2) free vortex region and 3) wall region. The vertical velocity profile through the center of the core shows the region of downdraft in addition to the core and the free vortex regions. The diameter of a vortex core is estimated to be $0.241D_0$ in horizontal direction, and $0.386D_0$ in vertical direction, that is, the vortex core is compressed in vertical direction.

The central downward flow as well as the entrainment above the ring agrees qualitatively with numerical simulation in spite of the large difference in the conditions.

Table 1 shows a comparison of present, observed (Wilson et al., 1984), numerical (Proctor, 1988) and experimental (Alahyari et al., 1995) microburst. Ave. is the averaged microburst reported by Wilson et al. (1984). Case A is the microburst that occurred on June 30, 1982. Out flow depth of the present is estimated from figure 5(a). We assume that height of the vortex core is the out flow depth

There is a great difference about the maximum horizontal velocity U_{max} between the present, the observation and other simulations. The present data is too small. The downdraft velocity is also small in

Parameter	Present	Wilson (1984) [a]		Proctor (1988)	Arahyari (1995)
		Ave.	Case A	case A	case A
$Umax/U_0$	0.3	1.15	1.63	2.02	3.12
Radial position of U_{max}, r/D_0	0.54	0.39	0.45	0.40	0.60
Out flow depth $/D_0$	0.39	0.25	0.19	0.19	0.25
The center of the vortex core	$r/D_0 = 0.6$	-	-	$r/D_0 = 0.45$	-
	$z/D_0 = 0.3$	-	-	$z/D_0 = 0.13$	-
Downdraft velocity W/D_0	0.19	1.15	1.44	1.15	2.47
Lifetime $t/(D_0/U_0)$	17.4	1.56	-	-	-

Table 1. Comparison of present and observed parameters for atmospheric microburst (Wilson et al., 1984) and numerical simulation (Proctor, 1988) and experimental simulation (Alahyari et al., 1995). Case A: June 30,1982,microburst. Ave.: Average of 70 observations (Wilson et al., 1984)

(a): Reference velocity and length are assumed to be equal to the Proctor's simulation

the present result. This is due to the absence of negative buoyancy that drives the downdraft in atmospheric microburst. The radial position of the maximum horizontal velocity, the outflow depth and the center position of the vortex core show good agreement with the present, the observation, the numerical simulation and the experimental simulation.

REFERENCES

Alahyari, A. & Longmire, E.K., 1995, "Dynamics of Experimentally Simulated Microbursts", *AIAA Journal*, vol.33, No.11, pp.2128-2136.

Fujita, T.T., 1985,*The Downburst*, Univ. Chicago Press

McCormack, P.D., 1973, *Physical Fluid Dynamics*, Academic Press, pp. 233.

Nagata, T. et al., 2000, "Laboratory simulation of downbursts", *20th Conference on Severe Local Storms*, , pp.409-412.

Orlandi, P. et al., 1993, "Vortex rings impinging on walls.", *Journal of Fluid Mechanics*, vol. 256, pp. 615-646.

Proctor, F.H., 1988, "Numerical simulation of an isolated microburst. Part Ⅰ: Dynamics and structure", *Journal of the Atmospheric Sciences*, vol. 45, No.21, pp.3137-3160.

Raffel, M. et al., 1998, *Particle Image Velocimetry*, Springer-Verlag Berlin Heidelberg.

Walker, J.D.A. et al., 1987, "The impact of a vortex ring on a wall.", *Journal of Fluid Mechanics*, vol.181, pp.99-140.

Wilson, J.W. et al., 1984, "Microburst Wind Structure and Evaluation of Doppler Radar for Airport Wind Shear Detection.", *Journal of Climate and Applied Meteorology*, vol.23, pp.898-915.

Yamada, H. et al., 1982, "Flowfield Produced by a Vortex Ring near a Plane Wall.", *Journal of the Physical Society of Japan*, vol.51, pp.1663-1670.